Extracting Electron-Ion Differential Scattering Cross Sections for Partially Aligned Molecules by Laser-Induced Rescattering Photoelectron Spectroscopy

Misaki Okunishi, Hiromichi Niikura, R. R. Lucchese, Toru Morishita, and Kiyoshi Ueda

Extracting Electron-Ion Differential Scattering Cross Sections for Partially Aligned Molecules by Laser-induced Rescattering Photoelectron Spectroscopy

Misaki Okunishi,[1] Hiromichi Niikura,[1,2] R.R. Lucchese,[1,3] Toru Morishita,[4,2] and Kiyoshi Ueda[1,*]

[1]*Institute of Multidisciplinary Research for Advanced Materials, Tohoku University, Sendai 980-8577, Japan*
[2]*PRESTO, Japan Science and Technology Agency,*
Sanbancho building, 5-Sanbancho, Chiyodaku, Tokyo 102-0075, Japan
[3]*Department of Chemistry, Texas A & M University, College Station, Texas 77843-3255, USA*
[4]*Department of Applied Physics and Chemistry, University of Electro-Communications,*
1-5-1 Chofu-ga-oka, Chofu-shi, Tokyo, 182-8585, Japan

We extract large-angle elastic differential cross sections (DCSs) for electrons scattering from partially aligned O_2^+ and CO_2^+ molecules using rescattering photoelectrons generated by infrared laser pulses. The extracted DCSs are in good agreement with those calculated theoretically, demonstrating that accurate DCSs for electron-ion scattering can be extracted from the laser-induced rescattering spectra, thus paving the way for dynamic imaging of chemical reactions by rescattering photoelectron spectroscopy.

When a molecule is exposed to an optical field whose magnitude matches the intra-molecular Coulombic fields, the molecule can be tunnel ionized, releasing an electron. This electron is then placed in the oscillating electric field of the laser and may be driven back to its parent ion and then recombine or rescatter. These processes form the core of the rescattering theory [1, 2] and are of current interest due to the possibility of using the returning electrons for self-imaging the target. When laser-induced photoelectrons are driven back to collide with the target ions, structural information about the target can be extracted from the recombination of the electrons and ions [3–6]. A ground-breaking study along this line was a demonstration that the outermost molecular orbital of the N_2 molecule can be extracted from the high-order harmonic generation (HHG) spectra using a tomographic procedure [4]. The extraction of the orbital wave function, however, even though extremely impressive, relies on a number of unconfirmed assumptions [7–11]. The realization of orbital tomography as a practical tool for retrieving structural information still awaits a careful theoretical investigation of the underlying assumptions.

In contrast to the wave of excitement and burst of exploitation that followed the discovery of HHG spectroscopy, angular distributions of rescattering photoelectrons are less studied. Rescattering photoelectron spectroscopy (RPS) can be regarded as a photoelectron diffraction measurement where the molecule being studied is both the source of the electrons and the scattering target. Noting the fact that electron diffraction with a pulsed electron gun is the cutting edge technique for retrieving time-evolved structures [12, 13], one can see that RPS offers great opportunities for determining molecular structure, with the benefit of achieving femto- to subfemtosecond temporal resolutions offered by the short laser pulses. In this connection it is worth noting the pioneering work by Meckel *et al.* [14], where they observed the rescattering photoelectrons from the dynamically aligned N_2 and O_2 molecules and analyzed them using a plane-wave approximation that is also used for the analysis of the HHG spectra [4].

Recently, it has been demonstrated, both theoretically and experimentally, that elastic differential cross sections (DCSs) for scattering of *free* electrons from *atomic* ions [15–18] can be accurately extracted from the momentum distributions of high-energy rescattering photoelectrons. In this Letter, we present the first demonstration of extracting DCSs of partially aligned molecules, in a wide range of electron momentum. Namely, we extract DCSs for electron scattering from partially aligned O_2^+ (CO_2^+) ground state ions, in the range 0.6(0.9)–3.3 a.u., from the angular distributions of laser-induced rescattered photoelectrons. The spectra are recorded for randomly oriented free molecules. The highest occupied molecular orbitals of O_2 and CO_2 are π_g symmetry and thus have the lobs at $\sim 45°$ relative to the molecular axis. As a result field ionization by the intense laser predominantly occurs for the molecules aligned at $\sim 45°$ relative to the laser polarization vector [19–21].

The main advantage for extracting DCSs in comparison with direct structure retrieval based on several assumptions such as the often-used plane-wave approximation is that the DCSs completely encapsulate electron-ion scattering and thus, in principle, can be used for more precise structure analysis [22] as well as the extraction of the charge distributions [23]. For comparison, we carry out *ab initio* calculations of DCSs for elastic scattering of *free* electrons from O_2^+ and CO_2^+. The *ab initio* DCSs are in good agreement with the extracted DCSs, confirming the validity of the extraction procedure. Furthermore, we find that the DCSs exhibit a rich structure that dramatically changes as the electron momentum changes in the range 0.7(0.9) − 3.3 a.u for O_2 (CO_2). This dramatic change reflects evolution of the double-slit-like multi-center interference fringes as a function of the electron momentum. Noting that the multi-center interference is sensitive to the bond lengths but cannot be precisely predicted by the plane-wave approxi-
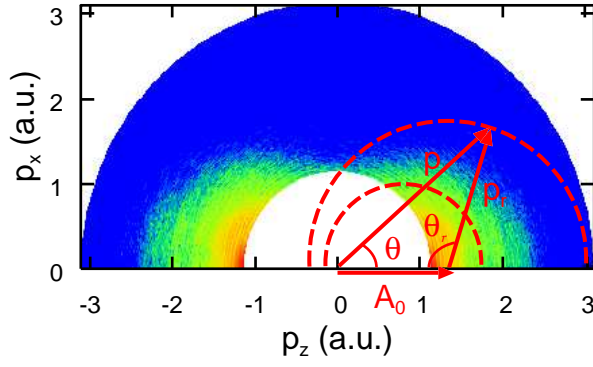
FIG. 1: (Color online) Laser-induced two-dimensional RPS spectrum for CO_2^+, at a laser intensity of 1.3×10^{14} W/cm^2. The intensity is plotted in logarithmic false color scale. The polarization direction of the linearly polarized lasers is along z-axis. The elastic scattering of a returning electron with momentum $\mathbf{p}_r$ is represented by an arc about the shifted center from the origin by $A_0 = p_r/1.26$. See text.

mation, the present DCSs measurement can be regarded as an important step towards dynamic imaging of chemical reactions by RPS.

In the experiments, we measured angle-resolved high-energy rescattering photoelectron spectra of randomly oriented O_2 and CO_2 with near-IR laser pulses from a 1 kHz amplified Ti:sapphire laser system. The laser beam was introduced into the vacuum chamber and focused by a $f = 60$ mm lens or a $f = 100$ mm mirror to ionize the effusively expanded sample molecules. We detected high-energy electrons with a linear time-of-flight spectrometer as a function of the angle between the laser (linear) polarization and the direction of emission of the electrons by rotating a $\lambda/2$ plate [24, 25]. The key point of the present experiments is that we covered a very wide range of laser intensities from 7×10^{13} W/cm^2 to 1.2×10^{15} W/cm^2 using three different pulse widths from the two different laser systems. At the lowest laser intensities, we used 100 fs laser pulse at a wavelength of 800 nm. For higher laser intensities, we used shorter pulse duration, 35 fs and 10 fs, at 785 nm (KMlabs, Dragon), in order to reduce the effect of depletion of the sample molecules. To generate the laser pulses of 10 fs duration, the pulses of 35 fs duration were compressed in an argon-filled hollow-core fiber. In this way, we could cover a wide range of recollision electron momentum up to 3.3 a.u.

To extract DCSs from the measured angle resolved RPS spectra, we apply the factorization formula of Morishita $et\ al.$ [15, 18]. For fixed-in-space molecules where the molecular axis makes angles $\hat{\mathbf{R}}' = \{\Theta', \Phi'\}$ with respect to the laser's polarization along the z-axis, high-energy photoelectron momentum distributions $S(\mathbf{p}, \hat{\mathbf{R}}')$ having the electron momentum of $\mathbf{p}$ can be expressed as

$$S(\mathbf{p}, \hat{\mathbf{R}}') = W(p_r, \hat{\mathbf{R}}')\sigma(\mathbf{p}_r, \hat{\mathbf{R}}'), \qquad (1)$$

where $\sigma(\mathbf{p}_r, \hat{\mathbf{R}}')$ is the fixed-in-space elastic DCS for the scattering of free electrons by the target ion with final momentum $\mathbf{p}_r = \{p_r, \theta_r, \phi_r\}$. Here $W(p_r, \hat{\mathbf{R}}')$ is the returning electron wave packet. Since the rescattering for the high-energy electrons occurs when the laser electric field is nearly zero, $i.e.$, the vector potential is close to the maximum value A_0, each electron will gain an additional drift momentum A_0 in the laser polarization direction. Moreover, the photoelectron having the highest energy of $10U_p$ has nearly the highest recollision energy of $\sim 3.2\ U_p$, where $U_p = A_0^2/4$ is the ponderomotive energy [26]. Thus, the recollision momentum is $p_r = \sqrt{2 \times 3.2 U_p} = 1.26 A_0$, and we have

$$\mathbf{p} = \pm A_0\,\hat{\mathbf{z}} + \mathbf{p}_r = \pm\,(p_r/1.26)\,\hat{\mathbf{z}} + \mathbf{p}_r \qquad (2)$$

where the "+" and "−" signs refer to electrons that, before scattering, are moving toward the ion from the $z > 0$ and the $z < 0$ directions, respectively [18, 23]. The relation in this equation is illustrated in Fig. 1 together with the definition of the angle θ_r. An analytical formulation of the factorization formula was recently derived [27]. For the lower energy part of the photoelectron spectra, the electrons may return to the ion core following a long or a short trajectory. It is shown, however, that the ratio between the recollision electron momentum p_r and the vector potential A does not change significantly from 1.26 and thus the relation in Eq. (2) can be used for those returning electrons that can be backscattered to emerge with energies higher than $4U_p$ [28].

Using a procedure similar to that used for analyzing HHG spectra in [29], we approximate the wave packet of Eq. (1) by $N(\Theta')\bar{W}(p_r)$, where $N(\Theta')$ is proportional to the Θ'-dependent ionization rate that can be measured [19] or calculated by the MO-ADK model [20] or the Siegert method [30]. The photoelectron momentum distribution for randomly oriented molecules is then obtained as

$$S(\mathbf{p}) = \bar{W}(p_r)\bar{\sigma}(p_r, \theta_r), \qquad (3)$$

where $\bar{\sigma}(p_r, \theta_r)$ is the DCS convoluted over the alignment angles, namely,

$$\bar{\sigma}(p_r, \theta_r) = \int N(\Theta')\bar{\sigma}(\mathbf{p}_r, \hat{\mathbf{R}}')d\hat{\mathbf{R}}'. \qquad (4)$$

The fixed-in-space DCS depends only on $\phi_r - \Phi'$ in the azimuthal angles, so that the electron spectra as well as the convoluted DCS exhibit cylindrical symmetry along the polarization axis.

The convoluted DCS, $\bar{\sigma}(p_r, \theta_r)$, depends very weakly on laser intensity via $N(\Theta')$. The relation between $\mathbf{p}_r$ and $\mathbf{p}$ is independent of laser intensity. We can thus integrate Eq. (3) over the focus volume to obtain the approximate formula:

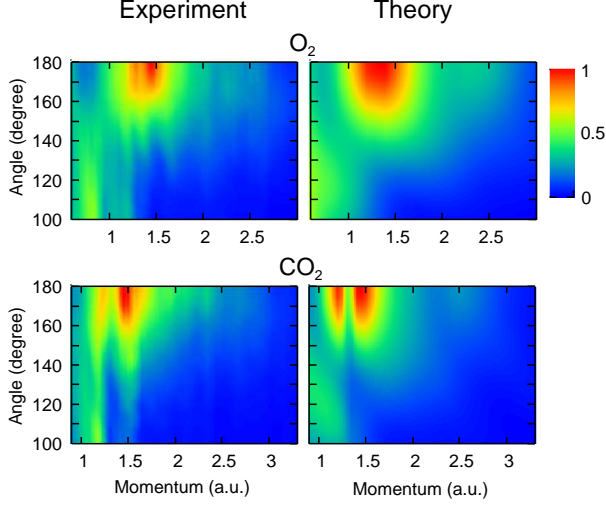$$S_{I_0}(\mathbf{p}) = \bar{W}_{I_0}(p_r)\bar{\sigma}(p_r, \theta_r), \qquad (5)$$

2

FIG. 2: (Color online) Experimental and theoretical elastic differential cross sections for scattering of free electrons from partially aligned O_2^+ and CO_2^+. The experimental data were normalized to the theoretical results at $\theta_r = 160°$. The theoretical results were obtained by a convolution with MO-ADK angle-dependent ionization rates. To smooth out the ATI peaks, the experimental DCSs are obtained by averaging the raw data over a bin of $\Delta p_r = 0.1$ a.u. and $\Delta\theta_r = 10°$.

where $S_{I_0}(\mathbf{p})$ is the volume-integrated photoelectron momentum distributions with a peak laser intensity of I_0 at the laser focus. $\bar{W}_{I_0}(p_r)$ is the volume-integrated wave packet, namely,

$$\bar{W}_{I_0}(p_r) = \rho \int_0^{I_0} \bar{W}_I(p_r) \left(-\frac{\partial V}{\partial I}\right) dI \qquad (6)$$

where $\bar{W}_I(p_r)$ is the wave packet for the laser pulse at the intensity I and ρ is the density of the target gas.

$S_{I_0}(\mathbf{p})$ of Eq. (5) describes the 2D electron momentum distributions measured experimentally, as shown in Fig. 1. Here, the spectrum was recorded for CO_2 at the lowest laser intensity of $I_0 = 1.3 \times 10^{14}$ W/cm^2. The precise laser intensity is not important. From such 2D spectra measured at many different laser intensities, we can extract the DCSs using Eq. (5).

The crucial function $\bar{W}$ cannot be obtained reliably from theory. Instead, for both O_2 and CO_2 we extracted $\bar{W}_I(p_r)$ from the experimental $S_{I_0}(\mathbf{p})$ employing the theoretical $\bar{\sigma}(p_r, \theta_r)$ at $\theta_r = 160°$. This normalization angle represents a compromise between an angle with weak dependence on p_r in the theoretical $\bar{\sigma}(p_r, \theta_r)$ and an angle with large cross sections. In other words, the extracted DCSs, $\bar{\sigma}(p_r, \theta_r)$, are normalized to the theoretical ones at $\theta_r = 160°$. Note that the θ_r variation of the experimental results are independent of the normalization angle, and the variation with p_r are only weakly dependent on this angle.

The resulting DCSs for CO_2 are shown in lower left

panel of Fig. 2. To construct this 2D map, we combined one 2D spectrum measured with 100 fs laser pulses ($I_0 = 1.3 \times 10^{14}$ W/cm^2), which covers $p_r = 0.9 - 1.25$ a.u., four spectra with 35 fs laser pulses ($I_0 = 1.5$, 1.8, 3.0, and 4.5×10^{14} W/cm^2), which cover $p_r = 1.25 - 2.3$ a.u., and two spectra with 10 fs laser pulses ($I_0 = 0.8$ and 1.2×10^{15} W/cm^2), which cover $p_r = 2.3 - 3.3$ a.u. There are some overlaps between the momentum ranges for different laser intensity pulses. In these cases, we used the lowest laser intensity to extract the DCSs, because the present procedure of the DCS extraction is the best for the largest momentum range. The corresponding DCSs for O_2 are shown in the upper left panel of Fig. 2, which includes our previous measurements [24, 25] at low laser intensities, as well as the present new ones. We used two 2D spectra with 100 fs laser pulse ($I_0 = 0.7$ and 1.3×10^{14} W/cm^2), which cover $p_r = 0.6 - 1.25$ a.u., two spectra with 35 fs laser pulses ($I_0 = 1.5$ and 2.0×10^{14} W/cm^2), which cover $p_r = 1.25 - 1.7$ a.u., and four spectra with 10 fs laser pulse ($I_0 = 0.35$, 0.6, 0.9, and 1.2×10^{15} W/cm^2), which cover $p_r = 1.7 - 3.3$ a.u.

To assist in and confirm the validity of the extraction of the DCSs as discussed above, we have carried out *ab initio* calculations for DCSs, $\sigma(\mathbf{p}_r, \hat{\mathbf{r}}')$ in Eq. (1). The calculations were performed using the Schwinger configuration interaction method [31], using interatomic distances fixed at their experimental equilibrium values [32, 33]. The augmented correlation-consistent polarized valence triple-ζ [34] one-electron basis set was used. The bound orbitals were obtained from valence complete active space self-consistent field calculations on the ground states of the neutral molecules and configuration interaction (CI) wave functions were used to describe the $^2\Pi_g$ ion ground states. In O_2 a full valence CI was used and in CO_2 the CI include all configuration state functions with up to five electrons in the virtual orbitals. The DCSs for electron-molecular ion scattering were obtained using single-channel calculations as discussed previously [35].

In the right-hand panels of Fig. 2 we show the resulting DCSs, $\bar{\sigma}(p_r, \theta_r)$, obtained from Eq. (4) using $N(\Theta')$ from the MO-ADK theory [20]. We also computed orientation averaged DCSs using angle-dependent ionization rates measured by Pavicic *et al.* [19]. In the case of CO_2^+, the resulting values of $\bar{\sigma}(p_r, \theta_r)$ did not agree with our measured DCSs as well as the $\bar{\sigma}(p_r, \theta_r)$ computed using the MO-ADK theory did. We note that the measured angle-dependent ionization rate for CO_2 [19] is much sharper than that calculated by the MO-ADK [20]. The angle-dependent ionization rate for O_2 calculated by the MO-ADK [20] agrees reasonably well with that measured by Pavicic *et al.* [19]. In the calculations, the dynamical alignment effects within the laser pulse before the ionization is not incorporated, because this effect is by far less significant than the geometrical alignment effects incorporated in the present calculation [36].

Both for O_2 and CO_2, the experimental DCSs, normal-

ized to the *ab initio* DCSs at $\theta_r = 160°$, are modulated as a function of electron momentum. The origin of these modulations can be found in the *ab initio* DCSs. Let us first look at the O_2 case. The modulation is significant especially at $\sim 180°$ where the electrons are backscattered. This modulation is mainly due to the double-slit-type interference. The returning electron wave packet is rescattered by the two O atoms, aligned at $45°$ relative to the polarization axis, and thus the back-scattered waves exhibit double slit interference [25]. The minimum at ~ 0.7 a.u. corresponds to the destructive interference and the maximum at ~ 1.2 a.u. corresponds to the constructive interference. These interference minimum/maximum are well reproduced by the present *ab initio* calculations. If we use a plane wave approximation, however, the minimum/maximum appear at different momenta, illustrating that proper scattering theory is indispensable for reproduction of the DCSs as well as rescattering photoelectron spectra. The minimum at ~ 1 a.u. in the backscattering of CO_2 illustrates the first observation of the destructive interference among the wave packets rescattered by the three atoms. The present *ab initio* theory reproduces this three center interference pattern. The structure in the DCSs for CO_2^+ at 1.2–1.4 a.u. is attributed to shape resonances in the $k\sigma_u$ and $k\pi_g$ continua which are found in our computed $\sigma(\mathbf{p}_r, \hat{\mathbf{r}}')$.

In summary, we have successfully extracted the large-angle elastic differential cross sections (DCSs) for scattering of free electrons by singly charged ions of partially aligned O_2 and CO_2 molecules from the momentum distributions of rescattering photoelectrons generated by infrared laser pulses. The extracted DCSs are in good agreement with *ab initio* results, confirming the validity of the extraction procedure. Noting that the double-slit-type interference includes information about the distances between the atoms of a molecule, the present result has a further implication that the rescattering electron spectroscopy is indeed potentially a powerful tool for determining the structure of molecules and thus may be employed for studying chemical reactions with a temporal resolution of femto- or subfemtoseconds and with atomic spatial resolution.

---

* ueda@tagen.tohoku.ac.jp
[1] K. Schafer *et al.*, Phys. Rev. Lett. **70**, 1599 (1993).
[2] P. B. Corkum, Phys. Rev. Lett. **71**, 1994 (1993).
[3] M. Lein *et al.*, Phys. Rev. Lett. **88**, 183903 (2002).
[4] J. Itatani *et al.*, Nature **432**, 867 (2004).
[5] T. Kanai *et al.*, Nature (London) **435**, 470 (2005).
[6] C. Vozzi *et al.*, Phys. Rev. Lett. **95**, 153902 (2005).
[7] S. Patchkovskii *et al.*, Phys. Rev. Lett. **97**, 123003 (2006).
[8] W.H.E. Schwarz, Angew. Chem. **45**, 1408 (2007).
[9] V.-H. Le *et al.*, Phys. Rev. A. **76**, 013414 (2007).
[10] J. Levesque *et al.*, Phys. Rev. Lett. **98**, 183903 (2007).
[11] Z.B. Walter *et al.*, J. Phys. Chem. **112**, 9439 (2008).
[12] A.H. Zewail, Annual Rev. of Phys. Chem., **57**, 65 (2006).
[13] J.R. Dwyer *et al.*, Phil. Trans. R. Soc. A **364**, 741-778 (2006).
[14] M. Meckel *et al.*, Science **320**, 1478 (2008).
[15] T. Morishita *et al.*, Phys. Rev. Lett., **100**, 013903 (2008).
[16] M. Okunishi *et al.*, Phys. Rev. Lett. **100**, 143001 (2008).
[17] D. Ray *et al.*, Phys. Rev. Lett. **100**, 143002 (2008).
[18] T. Morishita *et al.*, J. Phys. B: At. Mol. Opt. Phys. **42**, 105205 (2009).
[19] D. Pavicic *et al.*, Phys. Rev. Lett. **98**, 243001 (2007).
[20] S.-F. Zhao *et al.*, Phys. Rev. A **81**, 033423 (2010).
[21] S. Petretti *et al.*, Phys. Rev. Lett. **104**, 223001 (2010).
[22] J. Xu *et al.*, Phys. Rev. A **82**, 033403 (2010).
[23] T. Morishita *et al.*, J. Phys. Conf. Ser. **194**, 012011 (2009).
[24] M. Okunishi *et al.*, J. Phys. B: At. Mol. Opt. Phys. **41**, 201004 (2008).
[25] M. Okunishi *et al.*, Phys. Rev. Lett. **103**, 043001 (2009).
[26] G.G. Paulus *et al.*, J. Phys. B **27**, L703 (1994).
[27] O.I. Tolstikhin *et al.*, Phys. Rev. A **81**, 033415 (2010).
[28] Z. Chen *et al.*, Phys. Rev. A **79**, 033409 (2009).
[29] A.T. Le *et al.*, Phys. Rev. A **80**, 013401 (2009).
[30] P.A. Batishchev *et al.*, Phys. Rev. A **82**, 023416 (2010).
[31] R.E. Stratmann *et al.*, J. Chem. Phys. **104**, 8989 (1996).
[32] K.P. Huber and G. Herzberg, *Constants of Diatomic Molecules*, (Van Nostrand, New York, 1979).
[33] G. Herzberg, *Electronic Spectra and Electronic Structure of Polyatomic Molecules*, (Van Nostrand, New York, 1966).
[34] R.A. Kendall and T.H. Dunning, Jr., J. Chem. Phys. **96**, 6796 (1992).
[35] R.R. Lucchese and V. McKoy, Phys. Rev. A **24**, 770 (1981).
[36] X.M. Tong *et al.*, J. Phys. B: At. Mol. Opt. Phys. **38**, 333 (2005).